Physics Letters A 383 (2019) 328–337

Contents lists available at ScienceDirect

Physics Letters A

www.elsevier.com/locate/pla

General N-solitons and their dynamics in several nonlocal nonlinear Schrödinger equations

Jianke Yang

Department of Mathematics and Statistics, University of Vermont, Burlington, VT 05401, USA

ARTICLE INFO

Article history:
Received 4 December 2017
Received in revised form 4 June 2018
Accepted 31 October 2018
Available online 20 November 2018
Communicated by A.P. Fordy

Keywords:
Nonlocal NLS equations
Multi-solitons
Riemann–Hilbert solutions

ABSTRACT

General N-solitons in three recently-proposed nonlocal nonlinear Schrödinger equations are presented. These nonlocal equations include the reverse-space, reverse-time, and reverse-space–time nonlinear Schrödinger equations, which are nonlocal reductions of the Ablowitz–Kaup–Newell–Segur (AKNS) hierarchy. It is shown that general N-solitons in these different equations can be derived from the same Riemann–Hilbert solutions of the AKNS hierarchy, except that symmetry relations on the scattering data are different for these equations. This Riemann–Hilbert framework allows us to identify new types of solitons with novel eigenvalue configurations in the spectral plane. Dynamics of N-solitons in these equations is also explored. In all the three nonlocal equations, their solutions often collapse repeatedly, but can remain bounded or nonsingular for wide ranges of soliton parameters as well. In addition, it is found that multi-solitons can behave very differently from fundamental solitons and may not correspond to a nonlinear superposition of fundamental solitons.

1. Introduction

Integrable systems have been studied for many years [1–5]. Most such systems are local equations, i.e., the solution's evolution depends only on the local solution value and its local space and time derivatives. The Korteweg–de Vries equation and the nonlinear Schrödinger (NLS) equation are such examples.

A few years ago, a nonlocal reverse-space NLS equation

$$iq_t(x,t) + q_{xx}(x,t) + 2q^2(x,t)q^*(-x,t) = 0, \tag{1.1}$$

was proposed by Ablowitz and Musslimani [6]. Here the asterisk * represents complex conjugation. Although this equation is just a reduction of the Ablowitz–Kaup–Newell–Segur (AKNS) hierarchy, it is distinctive because the solution's evolution at location x depends on not only the local solution at x, but also the nonlocal solution at the distant position $-x$. That is, solution states at distant locations x and $-x$ are directly coupled, reminiscent of quantum entanglement between pairs of particles. Integrable equations of this type had not been paid attention before, which makes this nonlocal equation mathematically interesting. Regarding potential applications, this nonlocal equation was linked to an unconventional system of magnetics [7]. In addition, since this equation is parity-time ($\mathcal{PT}$) symmetric, i.e., it is invariant under the joint transformations of $x \to -x$, $t \to -t$ and complex conjugation, it is thus related to the concept of $\mathcal{PT}$ symmetry — a hot research area of contemporary physics [8].

Following its introduction, this reverse-space NLS equation was actively studied [6,9–17]. In addition, many other nonlocal integrable equations were reported and investigated [18–37]. These studies revealed interesting solution behaviors in nonlocal equations, such as finite-time solution blowup (i.e., collapsing) in fundamental solitons and general rogue waves of Eq. (1.1) [6,17] and the simultaneous existence of solitons and kinks in the nonlocal modified Korteweg–de Vries equation [30]. A connection between nonlocal and local equations was also discovered in [33], where it was shown that many nonlocal equations could be converted to local equations through transformations.

In this article, we study general N-solitons and their dynamics in the reverse-space NLS equation (1.1), as well as the reverse-time and reverse-space–time NLS equations,

$$iq_t(x,t) + q_{xx}(x,t) + 2q^2(x,t)q(x,-t) = 0, \tag{1.2}$$

and

$$iq_t(x,t) + q_{xx}(x,t) + 2q^2(x,t)q(-x,-t) = 0. \tag{1.3}$$

These equations can be derived from the following member of the AKNS hierarchy — the coupled Schrödinger equations [1,5]

$$iq_t + q_{xx} - 2q^2 r = 0, \tag{1.4}$$
$$ir_t - r_{xx} + 2r^2 q = 0. \tag{1.5}$$

E-mail address: jyang@math.uvm.edu.

https://doi.org/10.1016/j.physleta.2018.10.051
0375-9601/

Dynamics in these coupled Schrödinger equations without constraints between q and r has been analyzed in [5], and self-collapsing solitons as well as amplitude-changing solitons have been reported. Under reductions

$$r(x,t) = -q^*(-x,t), \tag{1.6}$$

$$r(x,t) = -q(x,-t), \tag{1.7}$$

and

$$r(x,t) = -q(-x,-t), \tag{1.8}$$

these coupled Schrödinger equations reduce to the reverse-space NLS equation (1.1), reverse-time NLS equation (1.2) and reverse-space–time NLS equation (1.3) respectively [6,26].

This article is motivated by a number of reasons. First, while solitons in the reverse-space NLS equation (1.1) have been investigated before [6,9,11,13], only the fundamental solitons were reported [6,9,11]. In [13], both fundamental and two-solitons were also reported; but those solutions are clearly incorrect, as was pointed out in [16]. In [10,15,16], "solitons" were also derived for Eq. (1.1); however, those solutions are not true solitons since they are not localized in space. Thus, despite the previous efforts, true multi-solitons in the reverse-space NLS equation (1.1) have never been found, which is surprising. This motivates us to derive general multi-soliton solutions in this nonlocal equation. As we will show, multi-solitons in this equation admit novel eigenvalue configurations in the spectral space, which give rise to new types of soliton structures, such as the two-soliton in Fig. 2 (bottom row). In addition, multi-solitons behave very differently from fundamental solitons.

Our second motivation is that, there has been no studies of solitons in the reverse-time NLS equation (1.2) and reverse-space–time NLS equation (1.3) to our best knowledge. The T-symmetric and ST-symmetric NLS equations studied in [16] and the reverse-t NLS equation studied in [37] are not the reverse-time and reverse-space–time NLS equations (1.2) and (1.3). In fact, those equations are just the nonlocal nonlinear diffusion equations analyzed in [33].

Our third motivation is that, it is helpful to put N-solitons of the three nonlocal equations (1.1)–(1.3) in the framework of inverse scattering and Riemann–Hilbert solutions, because in this framework, one can clearly see the novel symmetry relations in their scattering data, which strongly differ from those in the local (classical) NLS equation. In addition, this Riemann–Hilbert framework allows us to readily identify new types of solitons arising from new eigenvalue configurations in the spectral space, which can be more difficult to obtain by other methods (such as the Darboux transformation method and the bilinear method [11,13,15,16,37]).

In this article, we derive general N-solitons in the reverse-space, reverse-time and reverse-space–time NLS equations (1.1)–(1.3) using the inverse scattering and Riemann–Hilbert method. We show that N-solitons in these different equations can be derived from the same Riemann–Hilbert solutions of the AKNS hierarchy, except that symmetry relations on their scattering data differ from each other (and from those of the local NLS equation). From this Riemann–Hilbert framework, we discover new types of multi-solitons with novel eigenvalue configurations in the spectral plane. Since these eigenvalue configurations may not be split into groups of eigenvalues of fundamental solitons, we conclude that these multi-solitons may not be viewed as nonlinear superpositions of fundamental solitons. Dynamics of these solitons is further analyzed. In all the three nonlocal equations, we show that their solutions often collapse repeatedly, but can remain bounded or nonsingular for wide ranges of soliton parameters as well. In addition, we report that multi-solitons can behave very differently from fundamental solitons. For instance, in the reverse-time NLS equation (1.2), a two-soliton can move in opposite directions and repeatedly collapse, while the fundamental soliton is always stationary and nonsingular.

2. N-solitons for general coupled Schrödinger equations

Our basic idea to derive N-solitons in the reverse-space, reverse-time and reverse-space–time NLS equations (1.1)–(1.3) is to recognize that these equations are reductions of the coupled Schrödinger equations (1.4)–(1.5). Thus, we will start with the Riemann–Hilbert solutions of N-solitons for these coupled Schrödinger equations for given scattering data, then impose appropriate symmetry relations on this scattering data, which will yield N-solitons for the underlying nonlocal equations. Following this approach, we first consider N-solitons for the coupled Schrödinger equations (1.4)–(1.5), which will be done in this section.

The coupled Schrödinger equations (1.4)–(1.5) are a member of the AKNS hierarchy, and their Lax pairs are [38,39]

$$Y_x = MY, \quad Y_t = NY, \tag{2.1}$$

where

$$M = \begin{pmatrix} -i\zeta & q \\ r & i\zeta \end{pmatrix}, \quad N = \begin{pmatrix} -iqr - 2i\zeta^2 & iq_x + 2\zeta q \\ -ir_x + 2\zeta r & iqr + 2i\zeta^2 \end{pmatrix}. \tag{2.2}$$

For localized functions $q(x,t)$ and $r(x,t)$, the inverse scattering transform was developed in [38,39], and its modern Riemann–Hilbert treatment was developed in [2,40]. Following this Riemann–Hilbert treatment, N-solitons in this system were explicitly written down in [5] as

$$q(x,t) = 2i \left(\sum_{j,k=1}^{N} v_j \left(M^{-1}\right)_{jk} \bar{v}_k \right)_{12}, \tag{2.3}$$

and

$$r(x,t) = -2i \left(\sum_{j,k=1}^{N} v_j \left(M^{-1}\right)_{jk} \bar{v}_k \right)_{21}, \tag{2.4}$$

where

$$v_k(x,t) = e^{-i\zeta_k \Lambda x - 2i\zeta_k^2 \Lambda t} v_{k0}, \tag{2.5}$$

$$\bar{v}_k(x,t) = \bar{v}_{k0} e^{i\bar{\zeta}_k \Lambda x + 2i\bar{\zeta}_k^2 \Lambda t}, \tag{2.6}$$

M is a $N \times N$ matrix whose (j,k)-th element is given by

$$M_{jk} = \frac{\bar{v}_j v_k}{\bar{\zeta}_j - \zeta_k}, \quad 1 \le j,k \le N, \tag{2.7}$$

$\Lambda = \mathrm{diag}(1,-1)$, ζ_k are complex numbers in the upper half plane $\mathbb{C}_+$, $\bar{\zeta}_k$ are complex numbers in the lower half plane $\mathbb{C}_-$, and $v_{k0}, \bar{v}_{k0}$ are constant column and row vectors of length two respectively.

The above solutions can be written in a more compact form. Let us denote

$$v_{k0} = \begin{bmatrix} a_k \\ b_k \end{bmatrix}, \quad \bar{v}_{k0} = \begin{bmatrix} \bar{a}_k, \bar{b}_k \end{bmatrix}, \tag{2.8}$$

where $a_k, b_k, \bar{a}_k, \bar{b}_k$ are complex constants, and

$$\theta_k = -i\zeta_k x - 2i\zeta_k^2 t, \quad \bar{\theta}_k = i\bar{\zeta}_k x + 2i\bar{\zeta}_k^2 t. \tag{2.9}$$

Notice that M^{-1} in solutions (2.3)–(2.4) can be expressed as the transpose of M's cofactor matrix divided by $\det M$. Also recall that

the determinant of a matrix can be expressed as the sum of its elements along a row or column multiplying their corresponding cofactors. Hence solutions (2.3)–(2.4) can be rewritten as ratios of determinants [3,5]

$$q(x,t) = -2i\frac{\det F}{\det M}, \quad r(x,t) = 2i\frac{\det G}{\det M}, \tag{2.10}$$

where F and G are the following $(N+1)\times(N+1)$ matrices:

$$F = \begin{pmatrix} 0 & a_1 e^{\theta_1} & \dots & a_N e^{\theta_N} \\ \bar{b}_1 e^{-\bar{\theta}_1} & M_{11} & \dots & M_{1N} \\ \vdots & \vdots & \vdots & \vdots \\ \bar{b}_N e^{-\bar{\theta}_N} & M_{N1} & \dots & M_{NN} \end{pmatrix}, \tag{2.11}$$

and

$$G = \begin{pmatrix} 0 & b_1 e^{-\theta_1} & \dots & b_N e^{-\theta_N} \\ \bar{a}_1 e^{\bar{\theta}_1} & M_{11} & \dots & M_{1N} \\ \vdots & \vdots & \vdots & \vdots \\ \bar{a}_N e^{\bar{\theta}_N} & M_{N1} & \dots & M_{NN} \end{pmatrix}. \tag{2.12}$$

The reverse-space, reverse-time and reverse-space–time NLS equations (1.1)–(1.3) were obtained from the coupled system (1.4)–(1.5) under reductions (1.6)–(1.8). Each reduction leads to its own symmetry relations on the discrete scattering data $\{\zeta_k, \bar{\zeta}_k, v_{k0}, \bar{v}_{k0}, 1 \le k \le N\}$. For reasons which will become apparent in the next section, we call $\zeta_k, \bar{\zeta}_k$ eigenvalues and $v_{k0}, \bar{v}_{k0}$ eigenvectors in this paper. By deriving these symmetry relations for the eigenvalues and eigenvectors of the scattering data, N-soliton solutions of nonlocal equations (1.1)–(1.3) will be obtained directly from the above general N-soliton formulae (2.10). This will be done in the next section.

3. Symmetry relations of scattering data in the nonlocal NLS equations

We first present symmetry relations of the scattering data for the reverse-space, reverse-time and reverse-space–time nonlocal NLS equations (1.1)–(1.3), followed by their proofs. For this purpose, we introduce some notations. We define

$$\sigma_1 = \begin{bmatrix} 0 & 1 \\ 1 & 0 \end{bmatrix},$$

which is a Pauli spin matrix, and use the superscript 'T' to represent the transpose of a matrix. In addition, we use $\mathbb{R}_\pm$ to represent the sets of positive and negative real numbers respectively.

Theorem 3.1. *For the reverse-space NLS equation (1.1), if ζ is an eigenvalue, so is $-\zeta^*$. Thus, non-purely-imaginary eigenvalues appear as pairs $(\zeta, -\zeta^*)$, which lie in the same half of the complex plane. Symmetry relations on the eigenvectors are given as follows.*

1. *For a pair of non-purely-imaginary eigenvalues $(\zeta_k, \hat{\zeta}_k) \in \mathbb{C}_+$, $(\zeta_k, \hat{\zeta}_k) \notin i\mathbb{R}_+$, with $\hat{\zeta}_k = -\zeta_k^*$, their column eigenvectors v_{k0} and $\hat{v}_{k0}$ are related as $\hat{v}_{k0} = \sigma_1 v_{k0}^*$.*
2. *For a purely imaginary eigenvalue $\zeta_k \in i\mathbb{R}_+$, its eigenvector is of the form $v_{k0} = \left[1,\ e^{i\theta_k}\right]^T$, where θ_k is a real constant.*
3. *For a pair of non-purely-imaginary eigenvalues $(\bar{\zeta}_k, \hat{\bar{\zeta}}_k) \in \mathbb{C}_-$, $(\bar{\zeta}_k, \hat{\bar{\zeta}}_k) \notin i\mathbb{R}_-$, with $\hat{\bar{\zeta}}_k = -\bar{\zeta}_k^*$, their row eigenvectors $\bar{v}_{k0}$ and $\hat{\bar{v}}_{k0}$ are related as $\hat{\bar{v}}_{k0} = \bar{v}_{k0}^* \sigma_1$.*
4. *For a purely imaginary eigenvalue $\bar{\zeta}_k \in i\mathbb{R}_-$, its eigenvector is of the form $\bar{v}_{k0} = \left[1,\ e^{i\bar{\theta}_k}\right]$, where $\bar{\theta}_k$ is a real constant.*

Theorem 3.2. *For the reverse-time NLS equation (1.2), if ζ is an eigenvalue, so is $-\zeta$. Thus, eigenvalues appear as pairs $(\zeta, -\zeta)$, which lie on the opposite halves of the complex plane. For a pair of such eigenvalues $(\zeta_k, \bar{\zeta}_k)$ with $\zeta_k \in \mathbb{C}_+$ and $\bar{\zeta}_k = -\zeta_k \in \mathbb{C}_-$, their eigenvectors v_{k0} and $\bar{v}_{k0}$ are related as $\bar{v}_{k0} = v_{k0}^T$.*

Theorem 3.3. *For the reverse-space–time NLS equation (1.3), eigenvalues ζ_k can be anywhere in $\mathbb{C}_+$, and eigenvalues $\bar{\zeta}_k$ can be anywhere in $\mathbb{C}_-$. However, their eigenvectors must be of the forms*

$$v_{k0} = [1, \omega_k]^T, \quad \bar{v}_{k0} = [1, \bar{\omega}_k],$$

where $\omega_k = \pm 1$, and $\bar{\omega}_k = \pm 1$.

To put these results in perspective, we recall that for the local NLS equation, which is obtained from the coupled Schrödinger equations (1.4)–(1.5) under the reduction of $r(x,t) = -q^*(x,t)$, the symmetries of its scattering data are $\bar{\zeta}_k = \zeta_k^*$ and $\bar{v}_{k0} = v_{k0}^{*T}$ [1,2,5]. Thus, symmetry relations for the nonlocal NLS equations are very different from those of the local NLS equation. In particular, for the reverse-space and reverse-space–time NLS equations, eigenvalues in the upper and lower halves of the complex plane are completely independent. This independence allows for novel eigenvalue configurations, which will give rise to new types of multi-solitons. This will be demonstrated in the next section.

Before proving these theorems, we first establish a connection between the discrete scattering data for N-solitons, $\{\zeta_k, \bar{\zeta}_k, a_k, b_k, \bar{a}_k, \bar{b}_k, 1 \le k \le N\}$, and discrete eigenmodes in the eigenvalue problem $Y_x = MY$ and its adjoint eigenvalue problem $K_x = -KM$, i.e.,

$$Y_x = -i\zeta \Lambda Y + Q Y, \tag{3.1}$$

and

$$K_x = i\zeta K\Lambda - KQ, \tag{3.2}$$

where the potential matrix Q is

$$Q(x) = \begin{bmatrix} 0 & q(x,0) \\ r(x,0) & 0 \end{bmatrix}, \tag{3.3}$$

and $q(x,0)$, $r(x,0)$ are the initial conditions of functions $q(x,t)$ and $r(x,t)$. Indeed, it is known, from [5] for instance, that each subset $\{\zeta_k, a_k, b_k\}$ of the discrete scattering data, with $\zeta_k \in \mathbb{C}_+$, corresponds to a discrete eigenvalue ζ_k in the eigenvalue problem (3.1), whose discrete eigenfunction $Y_k(x)$ has the following asymptotics

$$Y_k(x) \longrightarrow \begin{bmatrix} a_k e^{-i\zeta_k x} \\ 0 \end{bmatrix}, \quad x \to -\infty, \tag{3.4}$$

$$Y_k(x) \longrightarrow \begin{bmatrix} 0 \\ -b_k e^{i\zeta_k x} \end{bmatrix}, \quad x \to +\infty. \tag{3.5}$$

Analogously, each subset $\{\bar{\zeta}_k, \bar{a}_k, \bar{b}_k\}$ of the discrete scattering data, with $\bar{\zeta}_k \in \mathbb{C}_-$, corresponds to a discrete eigenvalue $\bar{\zeta}_k$ in the adjoint eigenvalue problem (3.2), whose discrete eigenfunction $K_k(x)$ has the following asymptotics

$$K_k(x) \longrightarrow \begin{bmatrix} \bar{a}_k e^{i\bar{\zeta}_k x}, & 0 \end{bmatrix}, \quad x \to -\infty, \tag{3.6}$$

$$K_k(x) \longrightarrow \begin{bmatrix} 0, & -\bar{b}_k e^{-i\bar{\zeta}_k x} \end{bmatrix}, \quad x \to +\infty. \tag{3.7}$$

In view of this connection, in order to derive symmetry relations on the (discrete) scattering data, we will use symmetry relations of discrete eigenmodes in the eigenvalue problems (3.1)–(3.2), as we will do below. This symmetry derivation is easier than the standard one in [1,2,5], because it does not use details of the scattering theory for the underlying integrable equations.

Proof of Theorem 3.1. The reverse-space NLS equation (1.1) was derived from the coupled Schrödinger equations (1.4)–(1.5) under the reduction (1.6). With this reduction, the potential matrix Q is

$$Q(x) = \begin{bmatrix} 0 & q(x,0) \\ -q^*(-x,0) & 0 \end{bmatrix}, \tag{3.8}$$

which features the following symmetry,

$$Q^*(-x) = -\sigma_1^{-1} Q(x) \sigma_1. \tag{3.9}$$

Taking the complex conjugate to the eigenvalue equation (3.1), reversing x to $-x$, and utilizing the above potential symmetry, we get

$$\widehat{Y}_x = -i\hat{\zeta}\Lambda\widehat{Y} + Q\widehat{Y}, \tag{3.10}$$

where

$$\hat{\zeta} = -\zeta^*, \quad \widehat{Y}(x) = \alpha\sigma_1 Y^*(-x), \tag{3.11}$$

and α is an arbitrary complex constant. This equation shows that, if $\zeta_k \in \mathbb{C}_+$ is an eigenvalue of the scattering problem (3.1), so is $\hat{\zeta}_k \equiv -\zeta_k^* \in \mathbb{C}_+$. In addition, the eigenfunction $Y_k(x)$ of ζ_k and the eigenfunction $\widehat{Y}_k(x)$ of $\hat{\zeta}_k$ are related as in (3.11). Recall that the large-x asymptotics of ζ_k's eigenfunction $Y_k(x)$ has been given in Eqs. (3.4)–(3.5), and the large-x asymptotics of $\hat{\zeta}_k$'s eigenfunction $\hat{Y}_k(x)$ is the same as (3.4)–(3.5) but with ζ_k, a_k and b_k replaced by $\hat{\zeta}_k$, $\hat{a}_k$ and $\hat{b}_k$. Utilizing these asymptotics, the eigenfunction relation in Eq. (3.11) reveals that

$$\hat{a}_k = -\alpha b_k^*, \quad \hat{b}_k = -\alpha a_k^*, \tag{3.12}$$

i.e.,

$$\hat{v}_{k0} = -\alpha\sigma_1 v_{k0}^*. \tag{3.13}$$

If ζ_k is not purely imaginary, then its counterpart $\hat{\zeta}_k = -\zeta_k^*$ is a different eigenvalue. In this case, when the above $\hat{v}_{k0}$ expression is inserted into the N-soliton formulae (2.10), the constant $-\alpha$ cancels out and does not contribute to the solution. Thus, we can set $-\alpha = 1$ without loss of generality. Then, $\hat{v}_{k0} = \sigma_1 v_{k0}^*$, and part 1 of Theorem 3.1 is proved.

If ζ_k is purely imaginary, then $\hat{\zeta}_k = \zeta_k$. Thus, their eigenvectors are also the same, i.e., $\hat{v}_{k0} = v_{k0}$. Without loss of generality, we can scale the eigenvector v_{k0} so that its first element $a_k = 1$. Then, inserting $\hat{v}_{k0} = v_{k0}$ into Eq. (3.13), we find that $|\alpha| = 1$ and $v_{k0} = [1, -\alpha]^T$. Denoting $-\alpha = e^{i\theta_k}$, where θ_k is a real constant, we get $v_{k0} = [1, e^{i\theta_k}]^T$; hence part 2 of Theorem 3.1 is proved.

Repeating the above arguments on the adjoint eigenvalue problem (3.2), parts 3 and 4 of Theorem 3.1 can be similarly proved. □

Proof of Theorem 3.2. The reverse-time NLS equation (1.2) was derived from the coupled Schrödinger equations (1.4)–(1.5) under the reduction (1.7). With this reduction, the potential matrix Q is

$$Q(x) = \begin{bmatrix} 0 & q(x,0) \\ -q(x,0) & 0 \end{bmatrix}, \tag{3.14}$$

which features the following symmetry,

$$Q^T(x) = -Q(x). \tag{3.15}$$

Then, taking the transpose of the eigenvalue problem (3.1) and utilizing the above potential symmetry, we get

$$\overline{Y}_x = i\bar{\zeta}\,\overline{Y}\Lambda - \overline{Y}Q, \tag{3.16}$$

where

$$\bar{\zeta} = -\zeta, \quad \overline{Y}(x) = Y^T(x). \tag{3.17}$$

Eq. (3.16) means that $[\bar{\zeta}, \overline{Y}(x)]$ satisfies the adjoint eigenvalue equation (3.2). Thus, if $\zeta_k \in \mathbb{C}_+$ is an eigenvalue of the scattering problem (3.1), then $\bar{\zeta}_k = -\zeta_k \in \mathbb{C}_-$ is an eigenvalue of the adjoint scattering problem (3.2), and their eigenfunctions are related as in Eq. (3.17). Utilizing this eigenfunction relation as well as the large-x asymptotics of the eigenfunctions and adjoint eigenfunctions in Eqs. (3.4)–(3.7), we readily find that $\bar{a}_k = a_k$ and $\bar{b}_k = b_k$, i.e., $\bar{v}_{k0} = v_{k0}^T$. Theorem 3.2 is then proved. □

Proof of Theorem 3.3. The reverse-space–time NLS equation (1.3) was derived from the coupled Schrödinger equations (1.4)–(1.5) under the reduction (1.8). With this reduction, the potential matrix Q is

$$Q(x) = \begin{bmatrix} 0 & q(x,0) \\ -q(-x,0) & 0 \end{bmatrix}, \tag{3.18}$$

which features the symmetry,

$$Q(-x) = -\sigma_1^{-1} Q(x) \sigma_1. \tag{3.19}$$

Reversing x to $-x$ in the eigenvalue problem (3.1) and utilizing the above potential symmetry, we get

$$\widehat{Y}_x = -i\zeta\Lambda\widehat{Y} + Q\widehat{Y}, \tag{3.20}$$

where

$$\widehat{Y}(x) = \sigma_1 Y(-x). \tag{3.21}$$

This equation means that for any eigenvalue $\zeta_k \in \mathbb{C}_+$, if $Y_k(x)$ is its eigenfunction, so is $\widehat{Y}_k(x) = \sigma_1 Y(-x)$; thus $\widehat{Y}_k(x)$ and $Y_k(x)$ are linearly dependent, i.e.,

$$Y_k(x) = -\omega_k \sigma_1 Y_k(-x), \tag{3.22}$$

where ω_k is some constant. Utilizing this relation and the large-x asymptotics of the eigenfunction $Y_k(x)$ in Eqs. (3.4)–(3.5), we find that $a_k = \omega_k b_k$ and $b_k = \omega_k a_k$; thus $\omega_k = \pm 1$. Without loss of generality, we scale the eigenvector v_{k0} so that $a_k = 1$. Then, $b_k = \omega_k$, and $v_{k0} = [1, \omega_k]^T$.

Since Eq. (3.21) also means that for any eigenvalue $\bar{\zeta}_k \in \mathbb{C}_-$, if $K_k(x)$ is its adjoint eigenfunction, so is $\widehat{K}_k(x) = \sigma_1 K_k(-x)$. Hence utilizing this relation and the large-x asymptotics of the adjoint eigenfunction $K_k(x)$ in Eqs. (3.6)–(3.7), we can similarly show that $\bar{v}_{k0} = [1, \bar{\omega}_k]$, where $\bar{\omega}_k = \pm 1$. Theorem 3.3 is then proved. □

Before concluding this section, we point that it is also possible to impose (q, r) reductions (1.6)–(1.8) directly on the determinant solutions (2.10) in order to extract symmetry relations on the scattering data $\{\zeta_k, \bar{\zeta}_k, v_{k0}, \bar{v}_{k0}, 1 \le k \le N\}$. However, our derivation of these relations above is easier. In addition, this derivation is more insightful since it is in the inverse-scattering and Riemann–Hilbert framework.

4. Dynamics of N-solitons in the reverse-space NLS equation

To obtain general N-solitons in the reverse-space NLS equation (1.1), we only need to substitute the symmetry relations of the discrete scattering data in Theorem 3.1 into the general N-soliton formulae (2.10). The only thing we want to add is that, for a pair of non-imaginary eigenvalues $(\zeta_k, -\zeta_k^*) \in \mathbb{C}_+$, since we can scale the eigenvector v_{k0} of ζ_k so that $a_k = 1$ in Eq. (2.8), then using Theorem 3.1, we get

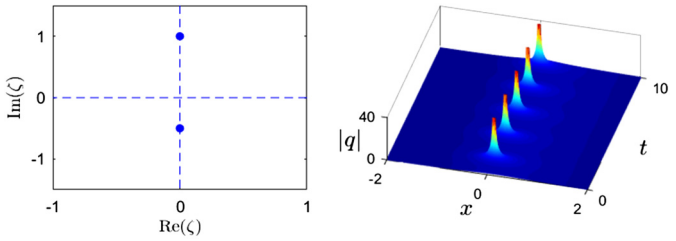

Fig. 1. A fundamental soliton (4.3) in the reverse-space NLS equation (1.1) with parameters (4.4). Left panel: locations of eigenvalues in the complex plane. Right panel: solution graph.

$$v_{k0} = [1, b_k]^T, \quad \hat{v}_{k0} = [b_k^*, 1]^T, \tag{4.1}$$

where $\hat{v}_{k0}$ is the eigenvector of eigenvalue $\hat{\zeta}_k \equiv -\zeta_k^*$, and b_k is a complex constant. Similarly, for a pair of non-imaginary eigenvalues $(\bar{\zeta}_k, -\bar{\zeta}_k^*) \in \mathbb{C}_-$, we can set their eigenvectors as

$$\bar{v}_{k0} = [1, \bar{b}_k], \quad \hat{\bar{v}}_{k0} = [\bar{b}_k^*, 1], \tag{4.2}$$

where $\bar{b}_k$ is another complex constant.

4.1. Fundamental solitons

First, we consider the fundamental (simplest) soliton solutions. These solutions correspond to a single pair of purely imaginary eigenvalues, $\zeta_1 = i\eta_1 \in i\mathbb{R}_+$, and $\bar{\zeta}_1 = i\bar{\eta}_1 \in i\mathbb{R}_-$, where $\eta_1 > 0$ and $\bar{\eta}_1 < 0$. Eigenvectors v_{10} and $\bar{v}_{10}$ of these eigenvalues are as given in Theorem 3.1, i.e., $v_{10} = \left[1, e^{i\theta_1}\right]^T$, and $\bar{v}_{10} = \left[1, e^{i\bar{\theta}_1}\right]$, where $\theta_1, \bar{\theta}_1$ are real constants. Substituting these expressions into the N-soliton formulae (2.10), we obtain the expression for the fundamental soliton in the reverse-space NLS equation (1.1) as

$$q(x,t) = \frac{2(\eta_1 - \bar{\eta}_1)e^{2\bar{\eta}_1 x + 4i\bar{\eta}_1^2 t + i\bar{\theta}_1}}{1 + e^{-2(\eta_1 - \bar{\eta}_1)x - 4i(\eta_1^2 - \bar{\eta}_1^2)t + i(\theta_1 + \bar{\theta}_1)}}, \tag{4.3}$$

which agrees with that derived in [6,9]. This soliton has four free real parameters, η_1, $\bar{\eta}_1$, θ_1 and $\bar{\theta}_1$ – the same number of free parameters as the fundamental soliton in the local NLS equation. However, the present soliton can not move in space regardless of the choice of parameter values, which contrasts that in the local NLS equation. Another general feature of this solution is that, if $\bar{\eta}_1 \neq -\eta_1$, i.e., $\bar{\zeta}_1 \neq -\zeta_1$, then it would breathe and periodically collapse in time at position $x = 0$. The period of this collapse is $\pi/[2(\eta_1^2 - \bar{\eta}_1^2)]$. To illustrate, we take parameter values

$$\eta_1 = 1, \quad \bar{\eta}_1 = -0.5, \quad \theta_1 = \pi/4, \quad \bar{\theta}_1 = 0. \tag{4.4}$$

In this case, the locations of eigenvalues ζ_1 and $\bar{\zeta}_1$ are shown in the left panel of Fig. 1, and the graph of the corresponding fundamental soliton is shown in the right panel of this figure.

If $\bar{\eta}_1 = -\eta_1$, i.e., $\bar{\zeta}_1 = -\zeta_1$, then as long as $\theta_1 + \bar{\theta}_1 \neq (2n+1)\pi$ for any integer n, this soliton will not collapse, and its amplitude $|q(x,t)|$ will not change with time [6,9].

4.2. Two-solitons

Now we consider two-solitons, which correspond to four eigenvalues, with $\zeta_1, \zeta_2 \in \mathbb{C}_+$ and $\bar{\zeta}_1, \bar{\zeta}_2 \in \mathbb{C}_-$. From Theorem 3.1, we see that (ζ_1, ζ_2) in $\mathbb{C}_+$ and $(\bar{\zeta}_1, \bar{\zeta}_2)$ in $\mathbb{C}_-$ are totally independent. Thus, these four eigenvalues can be arranged in 4 different configurations.

(1) $\zeta_1, \zeta_2 \in i\mathbb{R}_+$, and $\bar{\zeta}_1, \bar{\zeta}_2 \in i\mathbb{R}_-$.

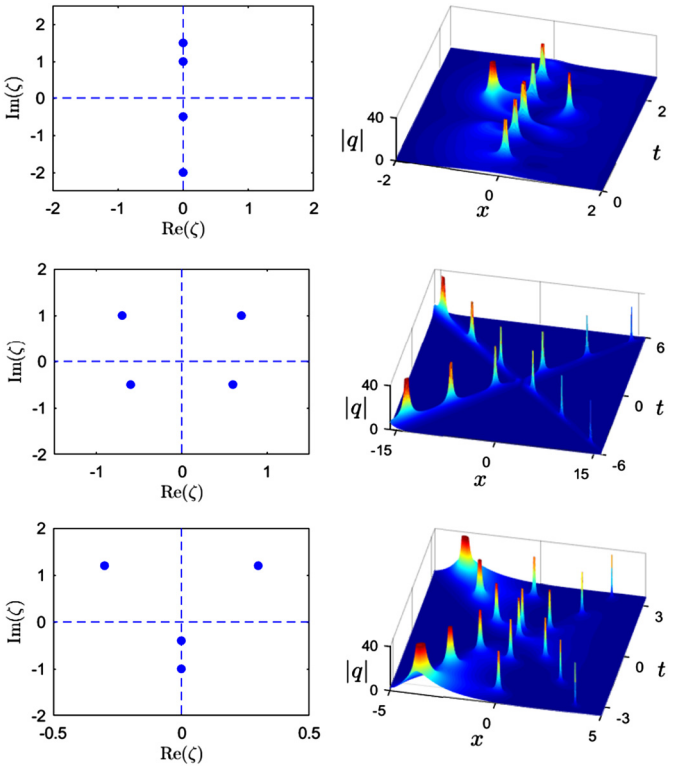

Fig. 2. Three examples of collapsing two-solitons in the reverse-space NLS equation (1.1). Parameters for these solitons (from top to bottom) are given in equations (4.6)–(4.7), (4.8)–(4.9), and (4.10)–(4.11), respectively. Left column: eigenvalue configurations; right column: solution graphs.

In this case, all four eigenvalues are purely imaginary. Thus, the two-soliton solution is obtained from the N-soliton formula (2.10) with $N = 2$, and the eigenvectors are given by Theorem 3.1 as

$$v_{k0} = \left[1, e^{i\theta_k}\right]^T, \quad \bar{v}_{k0} = \left[1, e^{i\bar{\theta}_k}\right], \quad k = 1, 2, \tag{4.5}$$

where $\theta_1, \theta_2, \bar{\theta}_1$ and $\bar{\theta}_2$ are free real constants. Together with the four free real constants in the eigenvalues, this two-soliton has 8 free real parameters. We find that this soliton does not move, similar to the fundamental soliton. In addition, if $\bar{\zeta}_1 \neq -\zeta_1$ or $\bar{\zeta}_2 \neq -\zeta_2$, then it would repeatedly collapse, mostly at $x = 0$, but occasionally at pairs of other spatial locations symmetric with respect to $x = 0$ as well. An example is shown in Fig. 2 (top row), where the parameters are chosen as

$$\zeta_1 = i, \quad \zeta_2 = 1.5i, \quad \bar{\zeta}_1 = -0.5i, \quad \bar{\zeta}_2 = -2i, \tag{4.6}$$

$$\theta_1 = \pi/4, \quad \theta_2 = 0, \quad \bar{\theta}_1 = 0, \quad \bar{\theta}_2 = \pi/2. \tag{4.7}$$

One may notice that the present eigenvalue configuration can be split into two pairs, $(\zeta_1, \bar{\zeta}_1)$ and $(\zeta_2, \bar{\zeta}_2)$, with each pair corresponding to the eigenvalue configuration of a fundamental soliton. This invites the view that the present two-soliton should describe the nonlinear superposition of two fundamental solitons. Indeed, the solution graph in the top row of Fig. 2 does more or less support this interpretation. However, this is not always the case. As we will see in the next section for the reverse-time NLS equation, even if a two-soliton's eigenvalue configuration can be split into groups of eigenvalues of fundamental solitons, this two-soliton may behave very differently from fundamental solitons and may not describe the nonlinear superposition of two fundamental solitons.

(2) $\zeta_1, \zeta_2 \notin i\mathbb{R}_+$, and $\bar{\zeta}_1, \bar{\zeta}_2 \notin i\mathbb{R}_-$.

This is an interesting case, where all four eigenvalues are non-imaginary. Then due to the eigenvalue symmetry of $(\zeta, -\zeta^*)$, we must have $\zeta_2 = -\zeta_1^*$, and $\bar{\zeta}_2 = -\bar{\zeta}_1^*$, which make up an eigenvalue quartet. This eigenvalue configuration has been suggested in [12], but the corresponding solitons have not been studied. Unlike case (1) above, these eigenvalues cannot be split into groups of imaginary-eigenvalue pairs of fundamental solitons; thus they generate a different type of solitons. We find that when $\mathrm{Im}(\zeta_1 + \bar{\zeta}_1) \neq 0$, these solitons generally collapse repeatedly at pairs of spatial locations which are symmetric with respect to $x = 0$. In addition, they move in two opposite directions as they collapse, which contrasts the stationary fundamental soliton in Fig. 1 and the stationary two-soliton in the top row of Fig. 2. To demonstrate, we take parameters as

$$\zeta_1 = -\zeta_2^* = 0.7 + i, \quad \bar{\zeta}_1 = -\bar{\zeta}_2^* = 0.6 - 0.5i, \tag{4.8}$$

$$b_1 = 1 + i, \quad \bar{b}_1 = 1 - 0.5i, \tag{4.9}$$

and the corresponding solution is plotted in the middle row of Fig. 2. Notice that in addition to moving and collapsing, another interesting feature of this soliton is that its amplitudes also change as it moves. Specifically, the amplitude of the right-moving wave decreases exponentially with time, while the amplitude of the left-moving wave increases exponentially with time. This exponential increase or decrease of amplitudes is due to $\mathrm{Re}(\zeta_1) \neq \mathrm{Re}(\bar{\zeta}_1)$. If $\mathrm{Re}(\zeta_1) = \mathrm{Re}(\bar{\zeta}_1)$, then this exponential change of amplitudes will disappear. Interestingly, the connections between eigenvalue relations (i.e., $\mathrm{Im}(\zeta_1 + \bar{\zeta}_1)$ or $\mathrm{Re}(\zeta_1 - \bar{\zeta}_1)$ being zero or not) and the two-soliton's collapsing or exponential change of amplitudes here are very similar to those in fundamental solitons of the reverse-space–time NLS equation, see the beginning of section 6.

(3) $\zeta_1, \zeta_2 \notin i\mathbb{R}_+$, and $\bar{\zeta}_1, \bar{\zeta}_2 \in i\mathbb{R}_-$.

This is an even more interesting configuration, where the two eigenvalues in the upper half plane are non-imaginary, but the two eigenvalues in the lower half plane are imaginary. Due to the eigenvalue symmetry of $(\zeta, -\zeta^*)$, the upper two non-imaginary eigenvalues must be related as $\zeta_2 = -\zeta_1^*$. This eigenvalue configuration has not been mentioned or reported before. Here again, the four eigenvalues cannot be split into groups of imaginary-eigenvalue pairs of fundamental solitons, and they create a new type of two-solitons which differ from those in cases (1) and (2). To illustrate the dynamics of these new solitons, we choose parameter values

$$\zeta_1 = -\zeta_2^* = 0.3 + 1.2i, \quad \bar{\zeta}_1 = -0.4i, \quad \bar{\zeta}_2 = -i, \tag{4.10}$$

$$b_1 = 1 + i, \quad \bar{\theta}_1 = -\pi/4, \quad \bar{\theta}_2 = -\pi. \tag{4.11}$$

This eigenvalue configuration and the corresponding two-soliton are presented in the bottom row of Fig. 2. This soliton features two waves traveling in opposite directions, plus another stationary wave in the middle (at $x = 0$). Both the traveling waves and the stationary wave collapse repeatedly over time. In addition, the amplitudes of the two traveling waves are changing, with the right-moving one decreasing with time and the left-moving one increasing with time. This two-soliton visually looks like a nonlinear superposition of a fundamental soliton as in Fig. 1, and a quartet-eigenvalue two-soliton as in the middle row of Fig. 2, even though its eigenvalue configuration does not suggest this visual appearance. We have also tested other choices of parameter values for this type of two-solitons and found that the solution patterns are largely similar to the one in the bottom row of Fig. 2, except that the periodic collapsing along the two traveling directions may disappear for certain choices of those parameters.

(4) $\zeta_1, \zeta_2 \in i\mathbb{R}_+$, and $\bar{\zeta}_1, \bar{\zeta}_2 \notin i\mathbb{R}_-$.

The fourth eigenvalue configuration is the opposite of case (3), where the upper two $\mathbb{C}_+$ eigenvalues are purely imaginary, and the lower two $\mathbb{C}_-$ eigenvalues are non-imaginary. Due to the eigenvalue symmetry of $(\zeta, -\zeta^*)$, the lower two non-imaginary eigenvalues are related as $\bar{\zeta}_2 = -\bar{\zeta}_1^*$. It is easy to check that solutions in this case can be linked to solutions of case (3). Specifically, suppose $q_4(x,t)$ is a solution of this case (4) with scattering data $S \equiv \{\zeta_k, \bar{\zeta}_k, v_{k0}, \bar{v}_{k0}, 1 \le k \le 2\}$, and $q_3(x,t)$ is a solution with scattering data S^*. Since the conjugated eigenvalues $\bar{\zeta}_1^*, \bar{\zeta}_2^*$ are in $\mathbb{C}_+$ and non-imaginary, and ζ_1^*, ζ_2^* are in $\mathbb{C}_-$ and imaginary, the solution $q_3(x,t)$ then belongs to case (3). It is easy to recognize that $q_4(x,t) = -q_3^*(-x,-t)$. Thus, solution behaviors in case (4) can be inferred from those of case (3) without the need of separate analysis.

4.3. Nonsingular and bounded two-solitons

The two-soliton solutions illustrated in Fig. 2 all repeatedly collapse and develop singularities. It is important to recognize that many other two-solitons do not collapse at all and can also remain bounded for all time. The existence of regular two-soliton solutions in a nonlocal three-wave interaction system has been reported in [22]. We will consider regular and bounded two-solitons in the reverse-space NLS equation (1.1) below.

For case (1) where all four eigenvalues are purely imaginary, we find that when $\bar{\zeta}_1 = -\zeta_1$ and $\bar{\zeta}_2 = -\zeta_2$, i.e., $\bar{\zeta}_k = \zeta_k^*$ $(k = 1, 2)$, the soliton could be bounded for all time for a wide range of parameter values of θ_1, θ_2, $\bar{\theta}_1$ and $\bar{\theta}_2$. Indeed, we can show analytically that if $\bar{\theta}_1 = -\theta_1$ and $\bar{\theta}_2 = -\theta_2$ (where $\bar{v}_{k0} = v_{k0}^{*T}$), the two-soliton is symmetric in x. Thus, this solution also satisfies the local NLS equation and is a NLS two-soliton, which is naturally bounded for all time. But if $\bar{\theta}_1 = -\theta_1 + \pi$ and $\bar{\theta}_2 = -\theta_2 + \pi$ (where $\bar{v}_{k0} = -v_{k0}^{*T}$), the solution is singular for all time. For other θ_1, θ_2, $\bar{\theta}_1$ and $\bar{\theta}_2$ values, the solution can remain bounded for all time, or repeatedly collapse. As an example of a bounded solution, we choose parameter values

$$\zeta_1 = -\bar{\zeta}_1 = i, \quad \zeta_2 = -\bar{\zeta}_2 = 2i, \tag{4.12}$$

$$\theta_1 = 0, \quad \theta_2 = \pi/2, \quad \bar{\theta}_1 = 0, \quad \bar{\theta}_2 = -\pi/3. \tag{4.13}$$

The corresponding two-soliton is plotted in the top row of Fig. 3. This solution breathes periodically but does not collapse. In addition, it is asymmetric in x and thus only satisfies the nonlocal NLS equation (1.1) but not the local NLS equation.

For case (2) where the four complex eigenvalues form a $(\zeta_1, -\zeta_1^*, \bar{\zeta}_1, -\bar{\zeta}_1^*)$ quartet, we find that when $\mathrm{Im}(\zeta_1 + \bar{\zeta}_1) = 0$, the two-soliton does not collapse (i.e., is nonsingular) for a wide range of b_1 and $\bar{b}_1$ values. As an example, we choose

$$\zeta_1 = -\zeta_2^* = 0.7 + i, \quad \bar{\zeta}_1 = -\bar{\zeta}_2^* = 0.6 - i, \tag{4.14}$$

$$b_1 = 1 + i, \quad \bar{b}_1 = 1, \tag{4.15}$$

and the corresponding soliton is shown in the middle row of Fig. 3. This soliton also features two waves moving in opposite directions (as in the middle row of Fig. 2), but remains regular and never collapses for all time. The two waves do become unbounded as $t \to \pm\infty$ though, which is caused by $\mathrm{Re}(\zeta_1) \neq \mathrm{Re}(\bar{\zeta}_1)$. If in addition, $\mathrm{Re}(\zeta_1) = \mathrm{Re}(\bar{\zeta}_1)$, so that $\bar{\zeta}_1 = \zeta_1^*$, then the soliton can become bounded for all time. To illustrate, we change $\bar{\zeta}_1$ in (4.14) to ζ_1^* and keep the other parameters the same, i.e., we choose the following parameter values,

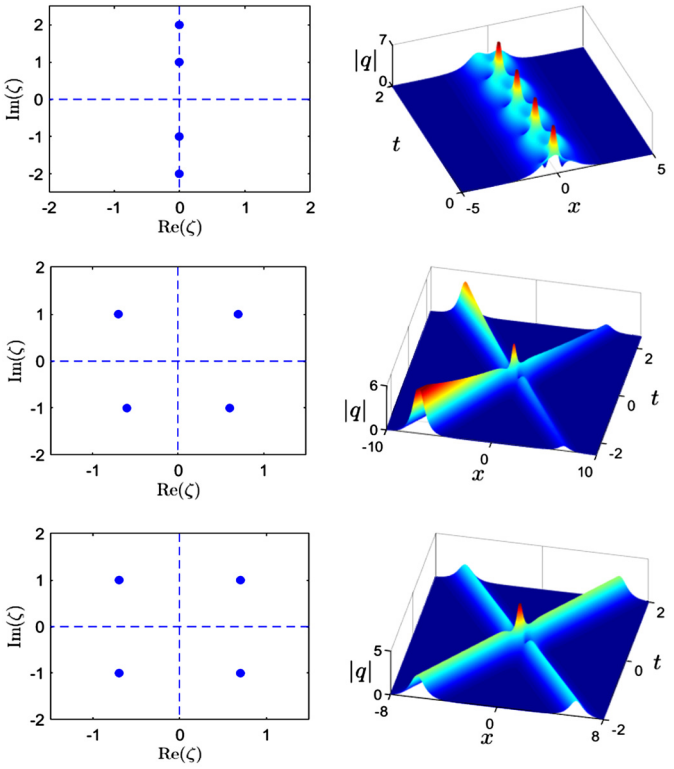

Fig. 3. Three examples of bounded or nonsingular two-solitons in the reverse-space NLS equation (1.1). Parameters for these solitons (from top to bottom) are given in equations (4.12)–(4.13), (4.14)–(4.15), and (4.16)–(4.17), respectively. Left column: eigenvalue configurations; right column: solution graphs.

$$\zeta_1 = -\zeta_2^* = 0.7 + i, \quad \bar{\zeta}_1 = -\bar{\zeta}_2^* = 0.7 - i, \tag{4.16}$$

$$b_1 = 1 + i, \quad \bar{b}_1 = 1, \tag{4.17}$$

and the corresponding two-soliton is shown in the bottom row of Fig. 3. This solution describes the elastic collision of two solitary waves, where the solitary waves fully recover their initial amplitudes and speeds after interaction. This behavior is very much like a two-soliton in the local NLS equation, even though the present solution is asymmetric in x and thus does not satisfy the local NLS equation. It is also noted that, unlike a two-soliton in the local NLS equation, each of the two solitary waves here does not satisfy the nonlocal reverse-space NLS equation (1.1). For other choices of parameter values, we can show analytically that when $\bar{\zeta}_1 = \zeta_1^*$ and $\bar{b}_1 = b_1^*$, the resulting two-soliton is always bounded for all time (since it is symmetric in x and thus also satisfies the local NLS equation). If $\bar{\zeta}_1 = \zeta_1^*$ but $\bar{b}_1 \neq b_1^*$, the solution is often bounded (as in the bottom row of Fig. 3), but can also collapse for certain choices of b_1 and $\bar{b}_1$ values.

For cases (3) and (4) with both non-imaginary and imaginary eigenvalues, we do not find nonsingular solutions.

From the above discussions, we see that two-solitons exhibit several new types of solutions which can repeatedly collapse or remain bounded, and their dynamics cannot be understood from the dynamics of fundamental solitons. Three- and higher-solitons can be studied similarly, and additional novel behaviors can be expected.

5. Dynamics of N-solitons in the reverse-time NLS equation

To obtain general N-solitons in the reverse-time NLS equation (1.2), we impose symmetry relations of discrete scattering data from Theorem 3.2 in the general N-soliton formulae (2.10). For a pair of discrete eigenvalues $(\zeta_k, \bar{\zeta}_k)$ with $\zeta_k \in \mathbb{C}_+$ and $\bar{\zeta}_k = -\zeta_k \in \mathbb{C}_-$, without loss of generality we scale the eigenvector v_{k0} of ζ_k so that $a_k = 1$ in (2.8). Then using Theorem 3.2, we get

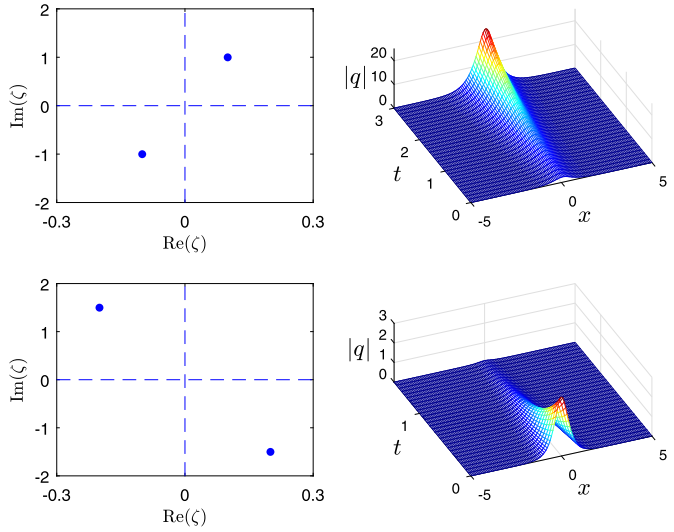

Fig. 4. Two fundamental solitons (5.2) in the reverse-time NLS equation (1.2). The parameter values (ζ_1, b_1) are $(0.1+i, 1+0.5i)$ in the upper row and $(-0.2+1.5i, 1)$ in the lower row. Left column: eigenvalue configurations; right column: solution graphs.

$$v_{k0} = [1, b_k]^T, \quad \bar{v}_{k0} = [1, b_k], \tag{5.1}$$

where b_k is a complex constant. This N-soliton has $2N$ free complex constants, $\{\zeta_k, b_k, 1 \le k \le N\}$, with $\zeta_k \in \mathbb{C}_+$.

The fundamental soliton is obtained when we set $N = 1$. In this case, simple algebra gives the analytical expression of this fundamental soliton as

$$q(x,t) = -4i\zeta_1 b_1 \frac{e^{-4i\zeta_1^2 t}}{e^{-2i\zeta_1 x} + b_1^2 e^{2i\zeta_1 x}}, \tag{5.2}$$

where ζ_1 and b_1 are free complex constants with $\zeta_1 \in \mathbb{C}_+$. This soliton does not move nor collapse. In addition, its amplitude grows or decays exponentially when ζ_1 is non-imaginary (it would grow/decay when ζ_1 is in the first/second quadrant of the complex plane $\mathbb{C}$). For two sets of parameter values, $(\zeta_1, b_1) = (0.1+i, 1+0.5i)$ and $(-0.2+1.5i, 1)$, the graphs of this soliton are illustrated in Fig. 4.

Two-solitons can be obtained from (2.10) under the above scattering-data relations. Surprisingly, even though the fundamental solitons never collapse, the two-solitons would collapse repeatedly if at least one of ζ_1 and ζ_2 is non-imaginary, and $\mathrm{Im}(\zeta_1) \neq \mathrm{Im}(\zeta_2)$. In addition, even though the fundamental solitons are stationary, the two-solitons would move in two opposite directions if ζ_1 and ζ_2 are not both purely imaginary. As an example, we choose parameter values as those in the two fundamental solitons of Fig. 4, i.e.,

$$\zeta_1 = 0.1 + i, \quad \zeta_2 = -0.2 + 1.5i, \quad b_1 = 1 + 0.5i, \quad b_2 = 1, \tag{5.3}$$

and the corresponding two-soliton is plotted in Fig. 5. Its repeated collapsing and two-way motion can be seen. Meanwhile, along the directions of motion, the wave amplitudes also decrease over time.

One may notice that the eigenvalue configuration of this two-soliton can be split into pairs of eigenvalues of fundamental solitons in Fig. 4, but its dynamics is totally different from that of the fundamental solitons. Thus, dynamics of two-solitons in the reverse-time NLS equation (1.2) is not a nonlinear superposition of

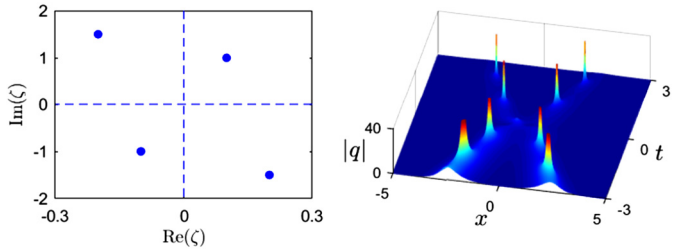

Fig. 5. A collapsing two-soliton in the reverse-time NLS equation (1.2). The parameter values are given in Eq. (5.3). Left panel: eigenvalue configuration; right panel: solution graph.

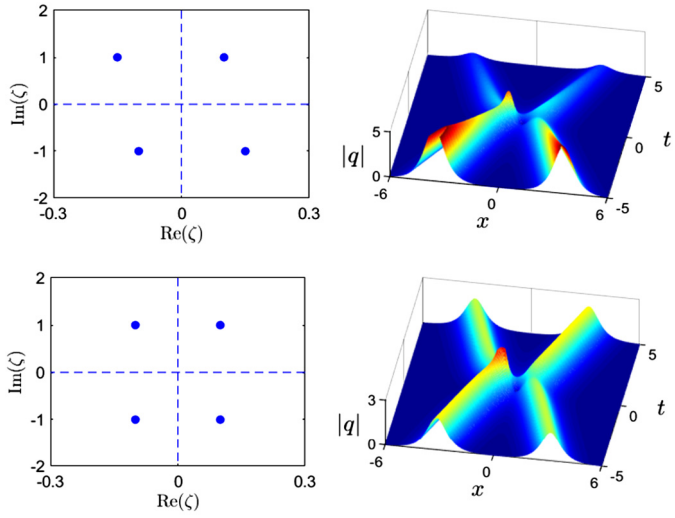

Fig. 6. Nonsingular and bounded two-solitons in the reverse-time NLS equation (1.2). Parameters for these solitons (from top to bottom) are given in equations (5.4) and (5.5). Left column: eigenvalue configurations; right column: solution graphs.

two fundamental solitons and cannot be predicted from the dynamics of fundamental solitons. This is similar to two-solitons in the reverse-space NLS equation (1.1), see Figs. 1–3.

Nonsingular and bounded two-solitons also exist for a wide range of parameter values. If $\mathrm{Im}(\zeta_1) = \mathrm{Im}(\zeta_2)$, then we find that the solitons often do not collapse. Such an example, with parameter choices

$$\zeta_1 = 0.1 + i, \quad \zeta_2 = -0.15 + i, \quad b_1 = 1 + 0.5i, \quad b_2 = 1, \tag{5.4}$$

is shown in the upper row of Fig. 6. This solution is regular, and its amplitudes decay exponentially over time. If in addition, $\mathrm{Re}(\zeta_1 + \zeta_2) = 0$, so that $\zeta_2 = -\zeta_1^*$, then the amplitudes would no longer decay, and a solution bounded for all time could be obtained. Indeed, we find that when $\zeta_2 = -\zeta_1^*$, the solution is bounded for almost all choices of b_1 and b_2 values. As an example, we change the above ζ_2 value to $-\zeta_1^*$, i.e.,

$$\zeta_1 = 0.1 + i, \quad \zeta_2 = -0.1 + i, \quad b_1 = 1 + 0.5i, \quad b_2 = 1. \tag{5.5}$$

The resulting two-soliton is plotted in the lower row of Fig. 6. This solution describes the elastic collision of two solitary waves and is bounded for all time, but each solitary wave itself is not a fundamental soliton since a fundamental soliton here does not move [see Eq. (5.2)].

Bounded two-solitons can also be obtained when ζ_1 and ζ_2 are both purely imaginary, and b_1, b_2 take certain ranges of complex values. For instance, the solution is bounded when $\zeta_1 = i$, $\zeta_2 = 1.5i$, $b_1 = b_2 = 1$.

6. Dynamics of N-solitons in the reverse-space–time NLS equation

To obtain general N-solitons in the reverse-space–time NLS equation (1.3), we impose symmetry relations of discrete scattering data from Theorem 3.3 in the general N-soliton formulae (2.10). Specifically, we let

$$v_{k0} = [1, \omega_k]^T, \quad \bar{v}_{k0} = [1, \bar{\omega}_k], \tag{6.1}$$

where $\omega_k = \pm 1$, and $\bar{\omega}_k = \pm 1$. This N-soliton has $2N$ free complex constants, $\{\zeta_k, \bar{\zeta}_k, 1 \le k \le N\}$, with $\zeta_k \in \mathbb{C}_+$ and $\bar{\zeta}_k \in \mathbb{C}_-$. In addition, each of ω_k and $\bar{\omega}_k$ has two choices between ± 1.

6.1. Fundamental solitons

For the fundamental soliton, we take $N = 1$. In this case, the analytical expression of this fundamental soliton is

$$q(x,t) = 2i(\bar{\zeta}_1 - \zeta_1)\frac{\bar{\omega}_1 e^{-2i\bar{\zeta}_1 x - 4i\bar{\zeta}_1^2 t}}{1 + \omega_1\bar{\omega}_1 e^{-2i(\bar{\zeta}_1-\zeta_1)x - 4i(\bar{\zeta}_1^2-\zeta_1^2)t}}, \tag{6.2}$$

where $\omega_1 = \pm 1$, $\bar{\omega}_1 = \pm 1$, and $\zeta_1 \in \mathbb{C}_+$, $\bar{\zeta}_1 \in \mathbb{C}_-$ are free. This soliton moves at velocity $V = -2\mathrm{Im}(\bar{\zeta}_1^2 - \zeta_1^2)/\mathrm{Im}(\bar{\zeta}_1 - \zeta_1)$. On the line $x = Vt$, its amplitude $|q|$ changes as

$$|q(t)| = 2|\bar{\zeta}_1 - \zeta_1|\frac{e^{\beta t}}{1 + \omega_1\bar{\omega}_1 e^{i\gamma t}}, \tag{6.3}$$

where

$$\beta = 2V\,\mathrm{Im}(\bar{\zeta}_1) + 4\mathrm{Im}(\bar{\zeta}_1^2), \tag{6.4}$$

$$\gamma = -2V\,\mathrm{Re}(\bar{\zeta}_1 - \zeta_1) - 4\mathrm{Re}(\bar{\zeta}_1^2 - \zeta_1^2). \tag{6.5}$$

The expressions for β and γ can be written more explicitly as

$$\beta = -8\frac{\mathrm{Im}(\zeta_1)\,\mathrm{Im}(\bar{\zeta}_1)\,\mathrm{Re}(\zeta_1 - \bar{\zeta}_1)}{\mathrm{Im}(\zeta_1 - \bar{\zeta}_1)}, \tag{6.6}$$

$$\gamma = -4|\zeta_1 - \bar{\zeta}_1|^2\frac{\mathrm{Im}(\zeta_1 + \bar{\zeta}_1)}{\mathrm{Im}(\zeta_1 - \bar{\zeta}_1)}. \tag{6.7}$$

Thus, when $\gamma \neq 0$, i.e., $\mathrm{Im}(\zeta_1 + \bar{\zeta}_1) \neq 0$, this soliton periodically collapses with period $2\pi/|\gamma|$. When $\beta \neq 0$, i.e., $\mathrm{Re}(\zeta_1 - \bar{\zeta}_1) \neq 0$, its amplitude grows or decays exponentially (depending on the sign of β). For the two sets of parameters

$$\zeta_1 = -0.3 + 0.9i, \quad \bar{\zeta}_1 = -0.2 - 0.4i, \quad \omega_1 = \bar{\omega}_1 = 1, \tag{6.8}$$

and

$$\zeta_1 = 0.4 + 0.9i, \quad \bar{\zeta}_1 = 0.3 - 0.6i, \quad \omega_1 = 1, \quad \bar{\omega}_1 = -1, \tag{6.9}$$

graphs of the two fundamental solitons are displayed in the upper and lower rows of Fig. 7 respectively. In the former case, the soliton moves at velocity $V \approx 1.0769$ (to the right). Along the line $x = Vt$, $|q|$ decreases exponentially at the rate of $e^{\beta t}$ with $\beta \approx -0.2215$, and collapses repeatedly with collapsing period $2\pi/|\gamma| \approx 2.4024$. In the latter case, the soliton moves at velocity $V = -1.44$ (to the left). Along the line $x = Vt$, $|q|$ increases exponentially at the rate of $e^{\beta t}$ with $\beta = 0.288$, and collapses repeatedly with collapsing period $2\pi/|\gamma| \approx 3.4752$.

If $\mathrm{Im}(\zeta_1 + \bar{\zeta}_1) = 0$, where $\gamma = 0$, then the above fundamental soliton will be regular (non-collapsing) when $\omega_1\bar{\omega}_1 = 1$. If in addition, $\mathrm{Re}(\zeta_1) = \mathrm{Re}(\bar{\zeta}_1)$, where $\beta = 0$, then this soliton will have constant amplitude for all time, similar to fundamental solitons in the local NLS equation.

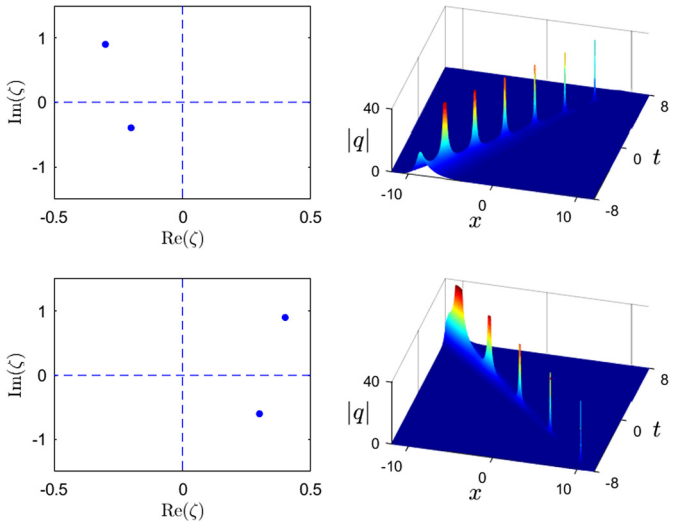

Fig. 7. Two fundamental solitons (6.2) in the reverse-space–time NLS equation (1.3). The parameter values for the upper and lower rows are given in Eqs. (6.8) and (6.9) respectively. Left column: eigenvalue configurations; right column: solution graphs.

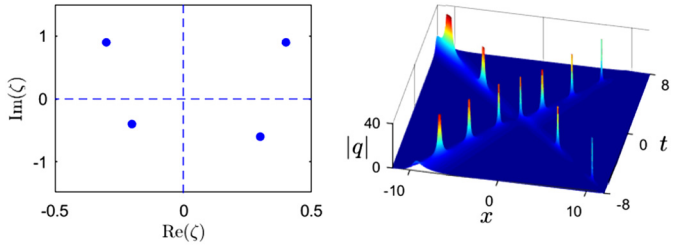

Fig. 8. A collapsing two-soliton in the reverse-space–time NLS equation (1.3). The parameter values are given in Eqs. (6.10)–(6.11). Left panel: eigenvalue configuration; right panel: solution graph.

6.2. Two-solitons

To get two-soliton solutions, we take $N = 2$ in the formula (2.10). Using the same parameters as in the two fundamental solitons of Fig. 7, i.e.,

$$\zeta_1 = -0.3 + 0.9i, \quad \bar{\zeta}_1 = -0.2 - 0.4i, \quad \omega_1 = \bar{\omega}_1 = 1, \tag{6.10}$$

$$\zeta_2 = 0.4 + 0.9i, \quad \bar{\zeta}_2 = 0.3 - 0.6i, \quad \omega_2 = 1, \quad \bar{\omega}_2 = -1, \tag{6.11}$$

the corresponding two-soliton is plotted in Fig. 8. This two-soliton moves in two directions, and collapses repeatedly as it moves. The amplitudes of the two moving waves change with time as well. When compared to the two fundamental solitons in Fig. 7, we see that this two-soliton does describe the nonlinear superposition between those two fundamental solitons, as the eigenvalue configuration of this two-soliton suggests (this eigenvalue configuration can be split into two groups corresponding to the eigenvalue configurations of the two fundamental solitons in Fig. 7). Thus, the reverse-space–time NLS equation (1.3) is the only nonlocal equation in this paper where a two-soliton is indeed a nonlinear superposition of two fundamental solitons.

The example shown in Fig. 8 is a repeatedly collapsing two-soliton. As with fundamental solitons in the previous subsection, nonsingular and bounded two-solitons exist as well under certain conditions of the soliton parameters. Specifically, when $\mathrm{Im}(\zeta_k + \bar{\zeta}_k) = 0$ and $\omega_k \bar{\omega}_k = 1$ $(k = 1, 2)$, the two-solitons will not collapse. If in addition, $\mathrm{Re}(\zeta_k) = \mathrm{Re}(\bar{\zeta}_k)$ $(k = 1, 2)$, so that $\bar{\zeta}_k = \zeta_k^*$, then the two-solitons will be bounded for all time. Notice that these conditions are the same as the conditions for individual

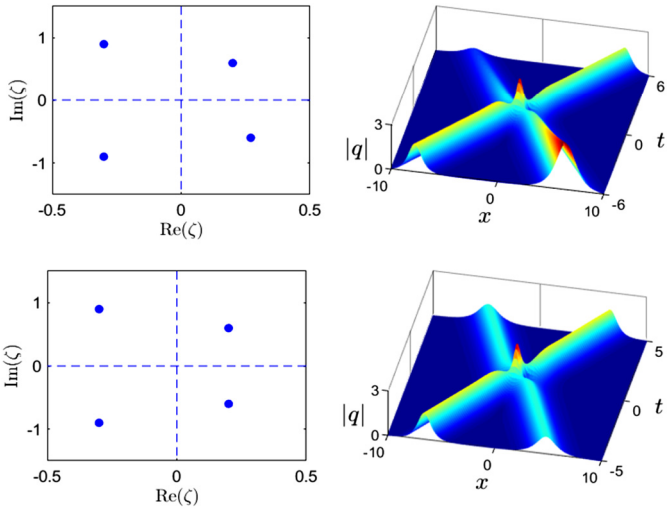

Fig. 9. Nonsingular and bounded two-solitons in the reverse-space–time NLS equation (1.3). The parameter values for the upper and lower rows are given in Eqs. (6.12)–(6.13) and (6.14)–(6.15) respectively. Left column: eigenvalue configurations; right column: solution graphs.

fundamental solitons to be regular and bounded. This is not surprising, since in the reverse-space–time NLS equation (1.3), a two-soliton is indeed a nonlinear superposition of two fundamental solitons, as we have mentioned earlier. As examples, we choose two sets of parameter values,

$$\zeta_1 = -0.3 + 0.9i, \quad \bar{\zeta}_1 = -0.3 - 0.9i, \quad \omega_1 = \bar{\omega}_1 = 1, \tag{6.12}$$

$$\zeta_2 = 0.2 + 0.6i, \quad \bar{\zeta}_2 = 0.27 - 0.6i, \quad \omega_2 = \bar{\omega}_2 = 1, \tag{6.13}$$

and

$$\zeta_1 = -0.3 + 0.9i, \quad \bar{\zeta}_1 = -0.3 - 0.9i, \quad \omega_1 = \bar{\omega}_1 = 1, \tag{6.14}$$

$$\zeta_2 = 0.2 + 0.6i, \quad \bar{\zeta}_2 = 0.2 - 0.6i, \quad \omega_2 = \bar{\omega}_2 = 1, \tag{6.15}$$

and the resulting two-solitons are displayed in the upper and lower rows of Fig. 9 respectively. For the first set of parameters where $\mathrm{Im}(\zeta_k + \bar{\zeta}_k) = 0$ and $\omega_k \bar{\omega}_k = 1$ $(k = 1, 2)$, the two-soliton does not collapse. Its right-moving wave does not decay in amplitude while its left-moving wave does, because $\mathrm{Re}(\zeta_1) = \mathrm{Re}(\bar{\zeta}_1)$ but $\mathrm{Re}(\zeta_2) \neq \mathrm{Re}(\bar{\zeta}_2)$. For the second set of parameters where $\bar{\zeta}_k = \zeta_k^*$ $(k = 1, 2)$, the two-soliton describes an elastic collision between two fundamental solitons and is bounded for all time.

7. Summary and discussion

In this article, we have derived general N-solitons in the reverse-space, reverse-time, and reverse-space–time nonlinear Schrödinger equations (1.1)–(1.3) from the Riemann–Hilbert solutions of the AKNS hierarchy. We have shown that symmetry relations of the scattering data in these nonlocal equations differ greatly from those of the local NLS equation, which lead to dramatically different solution behaviors in these nonlocal equations. We have found that solutions of these nonlocal equations often collapse repeatedly, but can remain bounded or nonsingular for wide ranges of soliton parameters. In addition, we have revealed that multi-solitons often do not describe a nonlinear superposition of fundamental solitons, and they can exhibit distinctive solution patterns which have not been seen before. These findings reveal the novel and rich soliton structures in the three nonlocal NLS equations (1.1)–(1.3), and they invite further investigations of solitons and multi-solitons in the other nonlocal equations.

The new symmetry properties of scattering data in these nonlocal equations also help resolve some open questions left over

in previous Riemann–Hilbert derivations of solitons. In that treatment, it was always assumed that the numbers of eigenvalues (known as zeros of the Riemann–Hilbert problem) in the upper and lower complex planes, counting multiplicity, were equal to each other [2,5,41]. A natural open question was: what would happen if the numbers of eigenvalues in $\mathbb{C}_+$ and $\mathbb{C}_-$ are not equal to each other? This question could not be addressed in the local (focusing) NLS equation, because in that case, eigenvalues always appear as conjugate pairs and thus always come in equal numbers in $\mathbb{C}_+$ and $\mathbb{C}_-$ [1–5]. However, in the reverse-space NLS equation (1.1) and reverse-space–time NLS equation (1.3), eigenvalues in $\mathbb{C}_+$ and $\mathbb{C}_-$ are totally independent (see Theorems 3.1 and 3.3). As a consequence, it is now possible for eigenvalues in $\mathbb{C}_+$ and $\mathbb{C}_-$ to appear in unequal numbers. To address this question, let us consider the simplest case in the reverse-space NLS equation (1.1), where there is a single pair of purely imaginary eigenvalues $(\zeta_1, \bar{\zeta}_1)$, but now both in $\mathbb{C}_+$. It is easy to verify that the previous fundamental soliton (4.3) still satisfies the reverse-space NLS equation (1.1) even though both ζ_1 and $\bar{\zeta}_1$ are in $i\mathbb{R}_+$. But in this case, this "fundamental soliton" is unbounded in space for all times, because it grows exponentially in either the positive or negative x directions. This example tells us that, when the Riemann–Hilbert problem has unequal numbers of zeros (eigenvalues) in the upper and lower complex planes, it would produce solutions which are unbounded in space (thus never solitons).

Acknowledgements

This material is based upon work supported by the Air Force Office of Scientific Research under award number FA9550-12-1-0244, and the National Science Foundation under award number DMS-1616122.

References

[1] M.J. Ablowitz, H. Segur, Solitons and Inverse Scattering Transform, SIAM, Philadelphia, 1981.
[2] S.P. Novikov, S.V. Manakov, L.P. Pitaevskii, V.E. Zakharov, Theory of Solitons, Plenum, New York, 1984.
[3] L. Takhtadjan, L. Faddeev, The Hamiltonian Approach to Soliton Theory, Springer Verlag, Berlin, 1987.
[4] M.J. Ablowitz, P.A. Clarkson, Solitons, Nonlinear Evolution Equations and Inverse Scattering, Cambridge University Press, 1991.
[5] J. Yang, Nonlinear Waves in Integrable and Non-integrable Systems, SIAM, Philadelphia, 2010.
[6] M.J. Ablowitz, Z.H. Musslimani, Phys. Rev. Lett. 110 (2013) 064105.
[7] T.A. Gadzhimuradov, A.M. Agalarov, Phys. Rev. A 93 (2016) 062124.
[8] V.V. Konotop, J. Yang, D.A. Zezyulin, Rev. Mod. Phys. 88 (2016) 035002.
[9] M.J. Ablowitz, Z.H. Musslimani, Nonlinearity 29 (2016) 915–946.
[10] X.Y. Wen, Z. Yan, Y. Yang, Chaos 26 (2016) 063123.
[11] X. Huang, L.M. Ling, Eur. Phys. J. Plus 131 (2016) 148.
[12] V.S. Gerdjikov, A. Saxena, J. Math. Phys. 58 (2017) 013502.
[13] S. Stalin, M. Senthilvelan, M. Lakshmanan, Phys. Lett. A 381 (2017) 2380–2385.
[14] V. Caudrelier, Stud. Appl. Math. 140 (2018) 3–26.
[15] K. Chen, D.J. Zhang, Appl. Math. Lett. 75 (2018) 82–88.
[16] M. Gürses, A. Pekcan, J. Math. Phys. 59 (2018) 051501.
[17] B. Yang, J. Yang, Rogue waves in the nonlocal $\mathcal{PT}$-symmetric nonlinear Schrödinger equation, Lett. Math. Phys. (2018), https://doi.org/10.1007/s11005-018-1133-5.
[18] M.J. Ablowitz, Z.H. Musslimani, Phys. Rev. E 90 (2014) 032912.
[19] Z. Yan, Appl. Math. Lett. 47 (2015) 61–68.
[20] A. Khara, A. Saxena, J. Math. Phys. 56 (2015) 032104.
[21] A.S. Fokas, Nonlinearity 29 (2016) 319–324.
[22] V.S. Gerdjikov, G.G. Grahovski, R.I. Ivanov, Theor. Math. Phys. 188 (2016) 1305–1321.
[23] Z.X. Xu, K.W. Chow, Appl. Math. Lett. 56 (2016) 72–77.
[24] J.L. Ji, Z.N. Zhu, Commun. Nonlinear Sci. Numer. Simul. 42 (2017) 699–708.
[25] S.Y. Lou, F. Huang, Sci. Rep. 7 (2017) 869.
[26] M.J. Ablowitz, Z.H. Musslimani, Stud. Appl. Math. 139 (2017) 7–59.
[27] V.S. Gerdjikov, G.G. Grahovski, R.I. Ivanov, Wave Motion 71 (2017) 53–70.
[28] Z.X. Zhou, Commun. Nonlinear Sci. Numer. Simul. 62 (2018) 480–488.
[29] Z.X. Zhou, Stud. Appl. Math. 141 (2018) 186–204.
[30] J.L. Ji, Z.N. Zhu, J. Math. Anal. Appl. 453 (2017) 973–984.
[31] J.G. Rao, Y. Cheng, J.S. He, Stud. Appl. Math. 139 (2017) 568–598.
[32] L.Y. Ma, S.F. Shen, Z.N. Zhu, J. Math. Phys. 58 (2017) 103501.
[33] B. Yang, J. Yang, Stud. Appl. Math. 140 (2018) 178–201.
[34] M. Gürses, Phys. Lett. A 381 (2017) 1791–1794.
[35] M.J. Ablowitz, X.D. Luo, Z.H. Musslimani, J. Math. Phys. 59 (2018) 011501; M.J. Ablowitz, B.F. Feng, X.D. Luo, Z.H. Musslimani, Stud. Appl. Math. 141 (2018) 267–307.
[36] B. Yang, Y. Chen, Commun. Nonlinear Sci. Numer. Simul. (2018), https://doi.org/10.1016/j.cnsns.2018.09.020.
[37] K. Chen, X. Deng, S.Y. Lou, D.J. Zhang, Stud. Appl. Math. 141 (2018) 113–141.
[38] V.E. Zakharov, A.B. Shabat, Zh. Èksp. Teor. Fiz. 61 (1971) 118, Sov. Phys. JETP 34 (1972) 62.
[39] M.J. Ablowitz, D.J. Kaup, A.C. Newell, H. Segur, Stud. Appl. Math. 53 (1974) 249.
[40] V.E. Zakharov, A.B. Shabat, Funkc. Anal. Prilozh. 13 (1979) 13–22, Funct. Anal. Appl. 13 (1979) 166–174.
[41] V.S. Shchesnovich, J. Yang, J. Math. Phys. 44 (2003) 4604–4639.